ISSN 0947-8396, Volume 100, Number 1

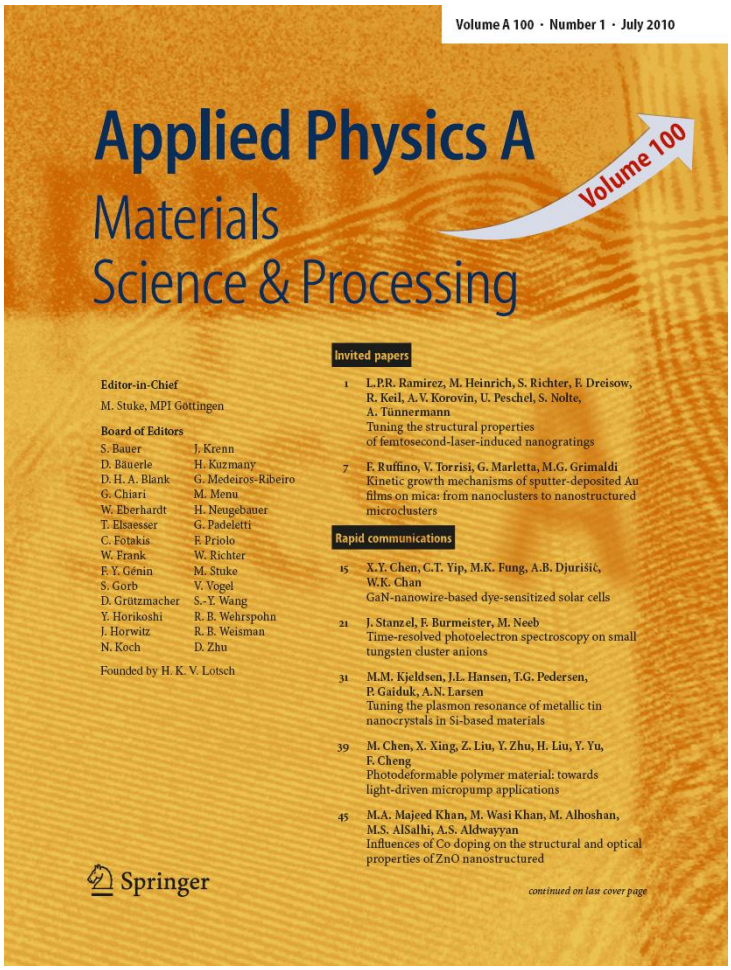

Appl Phys A (2010) 100: 151–157
DOI 10.1007/s00339-010-5589-0

Applied Physics A
Materials Science & Processing

Preparation and photoluminescence properties of silica-coated CuO nanowires

Changhyun Jin · Hyunsoo Kim · Chanseok Hong · Hyoun Woo Kim · Chongmu Lee

Received: 4 September 2009 / Accepted: 18 January 2010 / Published online: 18 March 2010

Abstract We have fabricated cupric oxide (CuO)-core/silica (SiO_x)-shell nanowires by using a two-step process: thermal oxidation and sputtering. The structure and photoluminescence (PL) properties of the core/shell nanowires has been investigated by using scanning electron microscopy, transmission electron microscopy, X-ray diffraction and PL analysis techniques. The CuO cores and the SiO_x shells of the as-synthesized nanowires have crystalline monoclinic CuO and amorphous SiO_x structures, respectively. The PL emission intensity of the CuO-core/SiO_x-shell nanowires has been increased but the emission peak position has not been nearly shifted by annealing in a nitrogen atmosphere, whereas the emission peak position has been shifted a lot from 510 to around 650 nm as well as the emission intensity has been increased by annealing in an oxygen atmosphere. In addition, the origin of the PL enhancement in the CuO-core/SiO_x-shell nanowires by annealing and the growth mechanism of the CuO nanowires have been discussed.

1 Introduction

It is essential to passivate one-dimensional (1D) nanostructures with insulating materials to avoid crosstalking between the building blocks of complex nanoscale circuits as well as to protect them from contamination and oxidation [1–9]. Passivation also offers many advantages such as substantial reduction of surface densities, prevention of the surface from adsorption of unwanted species, prevention of unnecessary charge injection, and partial screening of the external fields [10, 11]. In particular, passivation of nanowires is required in fabrication of field effect transistors and sensor devices based on nanowires. Various techniques have been reported to be used to form passivation layers on the 1D nanowire cores. These techniques include sol–gel processes, thermal heating, solution-based methods, chemical vapor deposition, and sputtering [12, 13]. On the other hand, SiO_x is known as one of the most suitable insulating material for nanowire passivation owing to its excellent insulating property, low dielectric constant, and high mechanical strength as well as compatibility with other materials widely used in integrated circuits (IC) fabrication. SiO_x is also optically transparent for light absorption or emission of semiconductor nanowires, resulting in minimal destruction of their intrinsic optical properties such as photoluminescence [14, 15].

CuO 1D nanostructures have recently attracted significant attention owing to their potential applications in electronic and optoelectronic devices such as high temperature superconductors, gas sensors, lithium batteries, optical switches, magnetoresistance materials, solar cells, electron field emitters, catalysts, and photovoltaic devices [16–20]. A variety of methods have been employed in synthesizing CuO 1D nanostructures, including thermal evaporation, thermal decomposition, electrospinning, thermal oxidation, sol–gel, solid–liquid arc discharge processes, templating methods, chemical vapor deposition, electrochemical methods, and hydrothermal treatment [21–28]. Among these methods, thermal oxidation is simple and offers synthesis of aligned CuO 1D nanostructures over a large area. CuO 1D nanostructures can be synthesized via an oxidation route by simply heating copper foils in an oxidative atmosphere without using catalysts.

C. Jin · H. Kim · C. Hong · H.W. Kim · C. Lee (✉)
Department of Materials Science and Engineering, Inha University, 253 Yonghyun-dong, Incheon 402-751, Republic of Korea
e-mail: cmlee@inha.ac.kr
Fax: +82-32-8625546

In this paper, we report influences of SiO_x coating and thermal annealing on the photoluminescence properties of CuO nanowires as well as the structure of SiO_x-coated CuO nanowires. The one-dimensional (1D) coaxial nanostructures were prepared by using two separate processes: thermal oxidation of copper (Cu) foils and sputtering of silicon in an atmosphere of argon and oxygen gas mixture.

2 Experimental

The synthesis of CuO-core/SiO_x-shell nanowires basically consists of two sequential processes: thermal oxidation of Cu foil in air for the core formation and sputter-deposition of SiO_x for the shell formation. First, a Cu foil with a thickness of 0.5 mm and a purity of 99.98% was cut into small rectangular-shaped pieces (2 cm × 2 cm). Prior to thermal oxidation, the Cu foil was dipped in diluted HCl solution for 10 s to remove native oxides and other contaminants. Next, the Cu foil was cleaned in an ultrasonicator with mixed solution of CH_3OH : acetone = 1 : 3 for 5 min and then in deionized water. After being dried by a nitrogen (N_2) gun, the Cu foil was placed in an alumina boat inside a quartz tube. The tube furnace was heated to 600°C at a heating rate of ∼5°C/min. After being kept in the air at 600°C for 5 h the sample was cooled down to room temperature. CuO nanowires were formed by thermal oxidation of the Cu foil surface without using Cu powders and metal catalysts at all.

Next, coating of the CuO nanowires with SiO_x was carried out by sputter-deposition of Si on the as-prepared CuO nanowires. The sputter-deposition was done at room temperature using a 99.999% Si target in a direct current (dc) magnetron sputtering system. Afterwards the vacuum chamber was evacuated to 1×10^{-3} mbar using a turbomolecular pump backed by a rotary pump. Depositions were carried out at a system pressure of 2×10^{-2} mbar and a dc power of 100 W in an Ar atmosphere. Subsequently, some of the prepared SiO_x-coated CuO nanowire samples were annealed in N_2 or O_2 atmosphere at 350°C for 1 h to see the influence of annealing on the PL properties of the coaxial nanowire structures.

The samples were then characterized by using glancing angle (0.5°) X-ray diffraction (XRD, X'pert MPD-Philips with Cu-K_α radiation), scanning electron microscopy (SEM, Hitachi S-4200), transmission electron microscopy (TEM, Phillips CM-200 equipped with an energy dispersive X-ray spectrometer (EDXS)). The high resolution TEM (HRTEM) images and the selected area electron diffraction (SAED) patterns were also taken on the same systems. The PL measurement was conducted at room temperature by using a He–Cd laser (325 nm) as an excitation source.

3 Results and discussion

Figures 1(a) and 1(b) show the SEM top view images of as-synthesized and SiO_x-coated CuO nanowires. Numerous nanorods with a diameter of a few tens or hundreds of nanometers and a length of a few tens of micrometers are observed in the SEM images. No distinct difference in morphology is found except that the coated nanowires are thicker than the uncoated ones. Figure 2 represents the XRD pattern of CuO-core/SiO_x-shell coaxial nanowires prepared by a two-step process: thermal oxidation of Cu foils at 600°C and sputter-deposition of SiO_x. The XRD patterns indicate that the CuO core consists of two types of cupric oxide phases: simple cubic Cu_2O (JCPDS 05-0667) and monoclinic CuO (JCPDS 48-1548). No diffraction peak of crystalline SiO_2 is observed in the diffraction pattern suggesting that the SiO_x shell layer is amorphous. The MoC peak is due to the MoC tape used to fix the nanowire sample during X-ray diffraction.

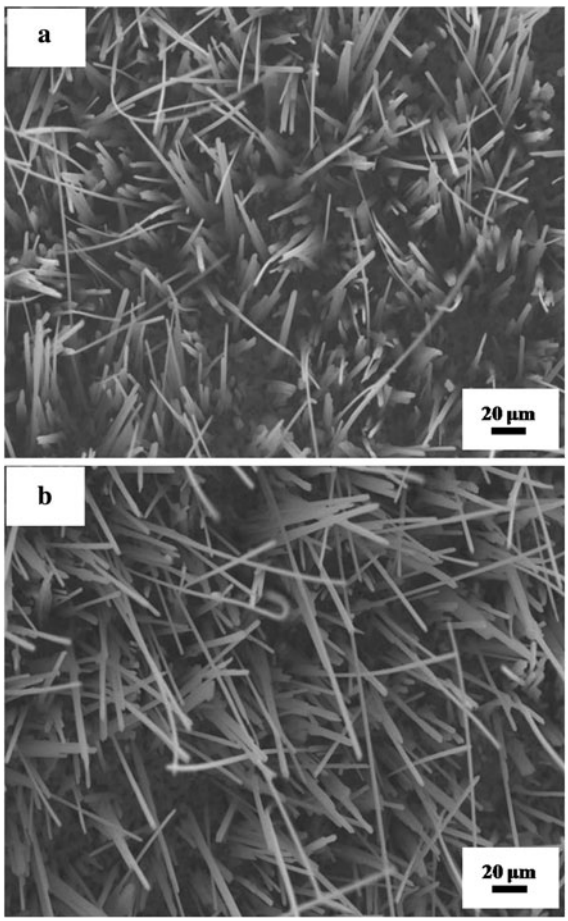

Fig. 1 Top view SEM images of (**a**) CuO nanowires synthesized by thermal oxidation of Cu foils at 600°C for 5 h and (**b**) SiO_x-coated CuO nanowires

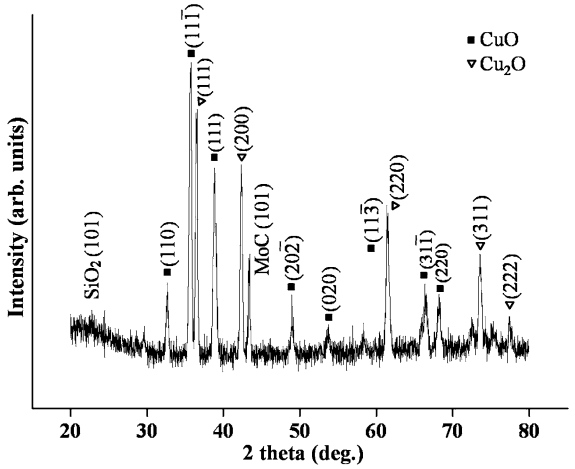

Fig. 2 XRD patterns of CuO-core/SiO_x-shell nanowires prepared by a two-step process: thermal oxidation of Cu foils at 600°C and sputter-deposition of SiO_x at 100 W for 1 h

The oxidation reaction of copper can be expressed as follows [29]:

$$4Cu + O_2 = 2\,Cu_2O, \tag{1}$$

$$2Cu_2O + O_2 = 4\,CuO. \tag{2}$$

When copper is oxidized in the air, the main product is Cu_2O as in reaction (1), and CuO forms slowly only through the second step of oxidation as in reaction (2) in which Cu_2O serves as a precursor to CuO. In other words, Cu_2O forms at a higher temperature or for a longer time than CuO. Both Cu_2O and CuO phases are reported to exist, but the Cu_2O phase is predominant at 600°C. According to the previous reports [29, 30], the surface of Cu foil is covered with a dense film of Cu_2O first and then CuO nanowires grow on the Cu_2O film. Therefore, it seems reasonable to suppose that the Cu_2O peaks in the XRD pattern for our nanowire samples are not contributed from the nanowires but from the Cu_2O layer underneath the nanowires. It may safely be assumed that the cores of the nanowires are comprised solely of the CuO phase.

The structure and crystallinity of the CuO nanowires were further characterized by using TEM. Figures 3(a) and 3(b) show the bright-field low- and high-magnification TEM images of a typical SiO_x-coated CuO nanowire, respectively. The inset of Fig. 3(b) shows that the nanowire is divided by a twin plane along the longitudinal axis. The enlarged image in Fig. 3(b) further confirms the bicrystallinity of the nanowire by showing a twin boundary separating the CuO core into two regions with different textures. Upon a close examination the directions of the textures in the two neighboring regions are somewhat different from each other, although the boundary between the two regions is not very clearly observable. The associated SAED pattern (Fig. 3(c)) was recorded with the incident electron

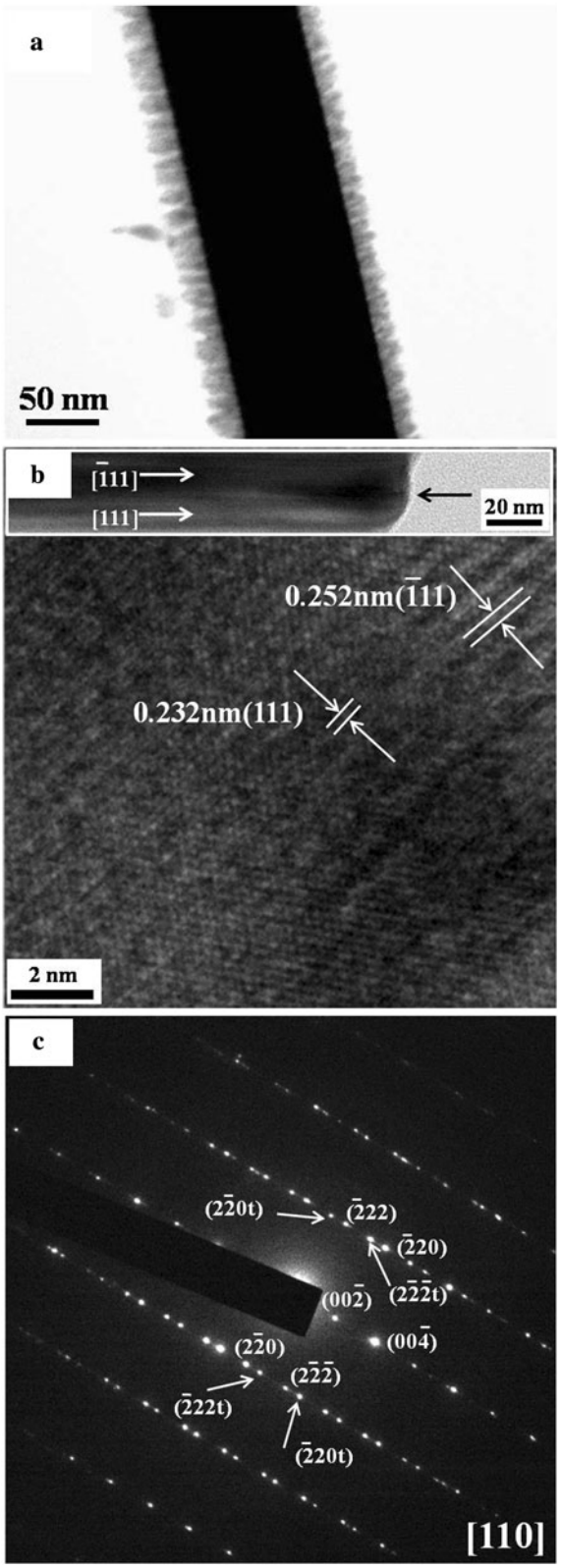

Fig. 3 (**a**) Low-magnification TEM image of a typical CuO-core/SiO_x-shell nanowire. (b) High-magnification TEM image of the nanowire. Indices without subscript *t* refer to the upperside of the nanowire shown in the inset, and indices with subscript *t* refer to the other side. The e-beam direction is parallel to the [110] axis. (**c**) The SAED pattern associated with the nanowire shown in (**b**)

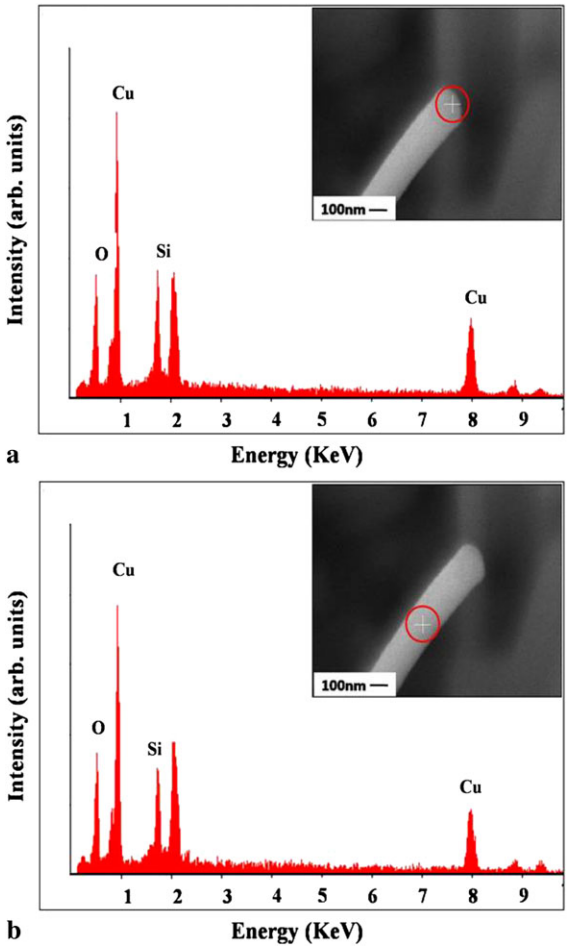

Fig. 4 EDX spectra of a typical CuO-core/SiO_x-shell nanowire synthesized by thermal oxidation of Cu foils and sputter-deposition of SiO_x: (**a**) at the tip of the nanowire as shown as the area marked '+' in the SEM image of the inset and (**b**) in the middle of the nanowire as shown as the area marked '+' in the SEM image of the inset

beam parallel to the [110] direction. The interplanar spacing of neighboring fringes of each side of the twin structure shown in Fig. 3(b) is 0.232 and 0.252 nm, which are in good agreement with the interplanar distances of {111} and {$\bar{1}$11} lattice plane families of monoclinic CuO with lattice parameters of $a = 0.469$ nm, $b = 0.342$ nm, $c = 0.512$ nm, and the interplanar angle of $\beta = 99.506°$ (JCPDS 48-1548). The mirror–image relationship between the two sets of direction spots confirms the formation of a crystalline structure within each nanowire. This result is in good agreement with the previous report [29].

The growth mechanism of CuO nanowires via a thermal oxidation route has been studied by many researchers, but it has not been well understood, yet. We performed EDX spectroscopy to reveal the growth mechanism of CuO nanowires. Figures 4(a) and 4(b) represent the EDX spectra of the tip and in the middle of a SiO_x-coated CuO naowire (the areas marked '+' in the SEM images of their insets), respectively. Almost no difference is found between the two spectra and no metal droplet is observed at the tip of the nanowire in the SEM image (the inset of Fig. 4(a)). One thing we can certainly say here based on the EDX analysis results is that vapor–liquid–solid (VLS) mechanism is not applicable to the growth of CuO nanowires by thermal oxidation since neither a metal catalyst was used in our synthesis process of CuO nanowires nor Cu droplets are observed at the tip of nanowires at all by SEM. As is well known, a catalyst droplet is commonly found at the tip of each nanowire grown via VLS mechanism. Jiang et al. [29] reported that the vapor–solid (VS) mechanism is responsible for the growth of CuO nanowires via a thermal oxidation route. However, Chen et al. [31] claimed that VS mechanism is also ruled out since evaporation of Cu, Cu_2O, or CuO is impossible to occur at the oxidation temperature below 700°C which is far lower than the melting points of Cu (1,083°C) and Cu_2O (1,243°C) and the decomposition temperature of CuO (1,124°C). Kumar et al. [32] reported that accumulation and relaxation of stress during the oxidation process is responsible for the CuO nanowire. In our opinion, the VS mechanism cannot be ruled out since evaporation of Cu or CuO can occur even below 700°C although its probability is low. The standard free energy changes for reactions (1) and (2) at 25 and 700°C are calculated to be negative as shown in Table 1, indicating that the reactions occur spontaneously in the temperature range from 25 to 700°C. The free energy values in Table 1 were calculated using the thermodynamic data in Table 2 [33]. Further study is necessary, but we surmise at the moment that both VS mechanism and stress relaxation mechanism are responsible for the growth of CuO nanowires by thermal oxidation.

Figures 5(a) and 5(b) show the low-magnification TEM image of a typical SiO_x-coated CuO nanowire and the associated EDXS concentration profiles of Cu, oxygen (O), and silicon (Si) along the diameter of the nanowire, respectively. A comparison of Cu and O concentration profiles indicates that the peak intensity ratio, i.e., the concentration ratio of Cu to O is closer to 2 than 1, suggesting that the Cu_2O phase is dominant over the CuO phase. This result is consistent with the XRD analysis result, yet the Cu_2O phase is contributed from the Cu_2O layer underneath the nanowires as was discussed earlier. Si elements are found to be present in the core region as well as in the shell region, although the Si concentration in the former is lower than that in the latter, which may be caused by penetration or diffusion of Si atoms into the CuO core during the sputtering process. Comparison of the Si concentration profile with the O profile suggests that Si elements mainly reside in the shell region. In contrast, O elements are found to be present in the shell region as well as in the core region, indicating that the phase in the shell region is SiO_x rather than pure Si, although the O concentration in the shell region is much lower than that in the core region. The O atoms in the shell region may originate from O impurities in the ambient gas of the sputter

Table 1 The standard free energy changes (ΔG^o) for reactions (1) and (2) at 700 and 25°C

	ΔG^o_{973} (Kcal/mole)	ΔG^o_{298} (Kcal/mole)
Reaction (1)	−23.617	−34.997
Reaction (2)	−14.087	−30.710

Table 2 Coefficients in free energy equations [32] ΔG_t (cal/mole) = $\Delta H_o + 2.303aT \log T + b \times 10^{-3}T^2 + c \times 10^5 T^{-1} + IT$

	ΔH_o	$2.303a$	b	C	I
$2Cu(c) + 1/2O_2(g) = Cu_2O(c)$	−40,550	−1.15	−1.10	−0.10	+21.92
$Cu(c) + 1/2O_2(g) = CuO(c)$	−37,740	−0.64	+1.40	−0.10	+24.87

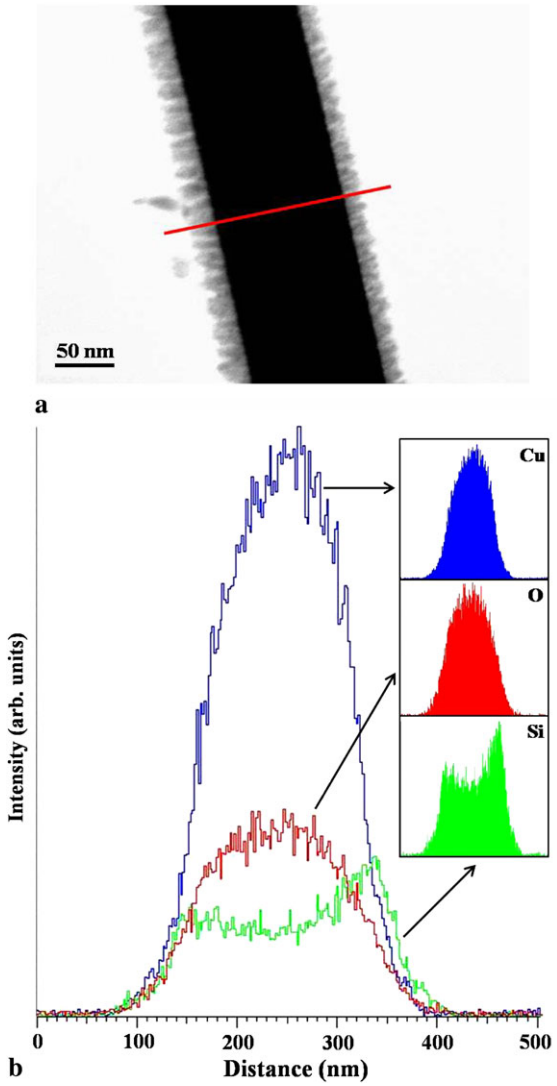

Fig. 5 EDX concentration profiles of as-synthesized CuO-core/SiO_x-shell nanowires

chamber and the Si target. Accordingly, these EDXS analysis results obtained by the line-scan along the diameter of the coated nanowire agree well with what can be expected for the SiO_x-coated CuO nanowires.

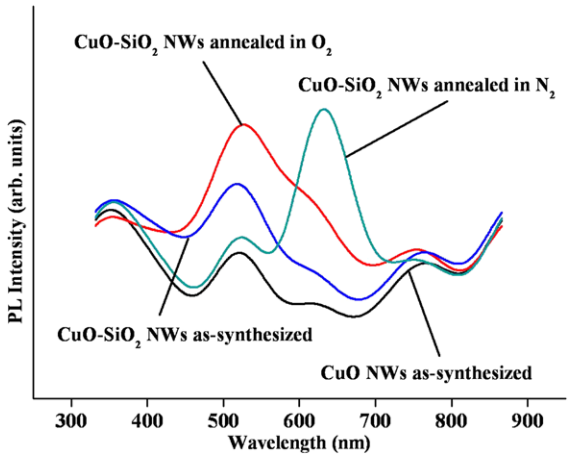

Fig. 6 Photoluminescence spectra of as-synthesized CuO nanowires, as-prepared SiO_x-coated CuO nanowires, the SiO_x-coated CuO nanowires annealed at 350°C in an Ar atmosphere, and the SiO_x-coated CuO nanowires annealed at 350°C in an O_2 atmosphere

As regards the PL properties of CuO materials there are very few reports on CuO materials. A violet emission band centered at 403 nm with a broad tail in the green spectral region was reported for sintered CuO whereas a broad emission band centered at 410 nm with a broad pronounced shoulder peak in the blue–green spectral region due to the defect-related emission formed during sparkling was reported for spark-processed CuO [34]. A broad emission band centered at 467 nm due to the quantum confinement effect was reported for CuO nanofilms [35, 36]. On the other hand, several luminescence bands in various silica glasses and nanowires with different peak wavelengths ranging from 288 to 653 nm were previously reported [37–46]. The 459 nm band was reported to be attributed to neutral oxygen vacancy and the 413.3 nm band to some intrinsic diamagnetic effect centers [47, 48].

Figure 6 represents the room temperature PL emission spectra of unannealed and annealed SiO_x-coated CuO nanowires along with as-synthesized CuO nanowires. We can see that the as-synthesized CuO nanowires have three different emission bands: a blue emission band centered at around 350 nm, a green emission band at around 510 nm,

and a red emission band at around 760 nm. The blue emission may originate from excitons and the other two may originate from deep level defects. The SiO_x-coated CuO nanowires show emissions somewhat stronger than that at the same wavelengths. The particularly large increase in the green emission intensity by SiO_x coating may be attributed to the increase in the concentration of deep level such as Si impurities formed in the CuO cores during Si sputtering.

The spectra also clearly show that the PL emission is enhanced by thermal annealing. The emission peak position has been shifted a lot from 510 to around 640 nm as well as the emission intensity has been increased by annealing in an N_2 atmosphere whereas the emission intensity has been increased but the emission peak position has not been shifted by annealing in an O_2 atmosphere. The new emission at around 640 nm generated by N_2 annealing may originate from the radiative recombination at the O vacancies during thermal annealing under O-free condition. On the other hand, the origin of the green emission at 540 nm from the coated nanowire sample annealed in an O_2 atmosphere is not clearly understood, but we surmise at the moment that the increase in the in the intensity of the green emission of the coated nanowires at 510 nm by annealing in O_2 is attributed to the increase in the concentration of the deep level defects such as color centers in the SiO_2 shell layer since the SiO_x in the shell layer is changed to SiO_2 by reacting with O_2 molecules in the O_2 atmosphere, although further detailed study is necessary.

4 Conclusions

We have fabricated CuO-core/SiO_x-shell 1D nanostructures by using a two-step process consisting of thermal oxidation of Cu foils and sputtering of Si. The nanowires synthesized at 600°C were comprised solely of the CuO phase. The Cu_2O phase detected by XRD and EDXS analyses were attributed to the Cu_2O layer underneath the nanowires. TEM and XRD analysis results reveal that the CuO-cores and the SiO_x-shells of the as-synthesized nanowires have crystalline monoclinic CuO and amorphous SiO_x structures, respectively. As regards the growth mechanism of CuO nanowires, both VS mechanism and stress relaxation mechanism are responsible for the growth of CuO nanowires by thermal oxidation.

PL measurements show that SiO_x coating increases the intensity of the emission, particularly the green emission, of CuO nanowires. The PL properties of the CuO-core/SiO_x-shell nanowires are found to strongly depend on the annealing atmosphere. The PL emission intensity of the CuO-core/SiO_x-shell nanowires has been increased and the emission peak position has not been nearly shifted by annealing in an N_2 atmosphere whereas the emission peak position has been shifted a lot from 510 to around 650 nm as well as the emission intensity has been increased by annealing in an O_2 atmosphere.

Acknowledgement This work was supported by Korea Science and Engineering Foundation through '2007 National Research Lab. Program'.

References

1. S. Aygun, D. Cann, Sens. Actuators B **106**, 837 (2005)
2. A. Cruccolini, R. Narducci, R. Palombari, Sens. Actuators B **98**, 227 (2004)
3. M. Frietsch, F. Zudock, J. Goschnick, M. Bruns, Sens. Actuators B **65**, 379 (2000)
4. T. Ishihara, M. Higuchi, T. Takagi, M. Ito, H. Nishiguchi, Y. Takita, J. Mater. Chem. **8**, 2037 (1988)
5. J. Tamaki, K. Shimanoe, Y. Yamada, Y. Yamamoto, N. Miura, N. Yamazoe, Sens. Actuators B **49**, 121 (1998)
6. L.S. Huang, S.G. Yang, T. Li, B.X. Gu, Y.W. Du, Y.N. Lu, S.Z. Shi, J. Cryst. Growth **260**, 130 (2004)
7. W. Wang, Y. Zhan, X. Wang, Y. Lui, C. Zheng, G. Wang, Mater. Res. Bull. **37**, 1093 (2002)
8. H. Wang, J.Z. Xu, J.J. Zhu, H.Y. Chen Preparation, of CuO nanoparticles by microwave irradiation. J. Cryst. Growth **244**, 88 (2002)
9. J.F. Xu, W. Ji, Z.X. Shen, S.H. Tang, X.R. Ye, D.Z. Jia, X.Q. Xin, J. Solid State Chem. **147**, 516 (1999)
10. B. Li, Y. Bando, D. Goldberg, Y. Uemura, Appl. Phys. Lett. **83**, 3999 (2003)
11. X. Liang, S. Tan, Z. Tang, N.A. Kotov, Langmuir **20**, 1016 (2004)
12. Y. Yin, Y. Lu, Y. Sun, Y. Xia, Nano Lett. **2**, 427 (2002)
13. H.W. Kim, J.W. Lee, C. Lee, M.A. Kebede, Polym. Adv. Technol. **20**, 246 (2009)
14. A. Schroeddter, H. Weller, R. Eritja, W.E. Ford, J.M. Wessels, Nano Lett. **281**, 225 (2004)
15. A. Pan, S. Wang, R. Liu, C. Li, B. Zou, Small **1**, 1058 (2005)
16. S. Aygun, D. Cann, Sens. Actuators B **106**, 837 (2005)
17. A. Cruccolini, R. Narducci, R. Palombari, Sens. Actuators B **98**, 227 (2004)
18. M. Frietsch, F. Zudock, J. Goschnick, M. Bruns, Sens. Actuators B **65**, 379 (2000)
19. T. Ishihara, M. Higuchi, T. Takagi, M. Ito, H. Nishiguchi, Y. Takita, J. Mater. Chem. **8**, 2037 (1988)
20. J. Tamaki, K. Shimanoe, Y. Yamada, Y. Yamamoto, N. Miura, N. Yamazoe, Sens. Actuators B **49**, 121 (1998)
21. L.S. Huang, S.G. Yang, T. Li, B.X. Gu, Y.W. Du, Y.N. Lu, S.Z. Shi, J. Cryst. Growth **260**, 130 (2004)
22. W. Wang, Y. Zhan, X. Wang, Y. Lui, C. Zheng, G. Wang, Mater. Res. Bull. **37**, 1093 (2002)
23. H. Wang, J.Z. Xu, J.J. Zhu, H.Y. Chen, J. Cryst. Growth **244**, 88 (2002)
24. J.F. Xu, W. Ji, Z.X. Shen, S.H. Tang, X.R. Ye, D.Z. Jia, X.Q. Xin, J. Solid State Chem. **147**, 516 (1999)
25. G. Xu, Y. Liu, G. Xu, G. Wang, Mater. Res. Bull. **37**, 2365 (2002)
26. T. Yu, X. Zhao, Z.X. Shen, Y.H. Wu, W.H. Su, J. Cryst. Growth **268**, 590 (2004)
27. P. Raksa, S. Kittikunodom, S. Choopun, T. Chairungsri, P. Mangkorntong, N. Mankorntong, CMU J. (Special Issue on Nanotechnology) **4**, 1 (2005)
28. C.H. Xu, C.H. Woo, S.Q. Shi, Chem. Phys. Lett. **399**, 62 (2004)
29. X. Jiang, T. Herricks, Y. Xia, Nano Lett. **2**, 1333 (2002)
30. R.C. Wang, C.H. Li, Cryst. Growth Des. **9**, 2229 (2009)

31. J.T. Chen, F. Zhang, J. Wang, G.A. Zhang, B.B. Miao, X.Y. Fan, D. Yan, P.X. Yan, J. Alloys Compd. **454**, 268 (2008)
32. M. Kumar, A.K. Srivastava, P. Tiwari, R.V. Nandedkar, J. Phys.: Condens. Matter. **16**, 670 (2006)
33. R.C. Weast (ed.), *CRC Handbook of Chemistry and Physics*, 58th edn. (CRC Press, Boca Raton, 1978), D-67
34. D.W. Snoke, A.J. Shields, M. Cardona, Phys. Rev. B **45**, 11693 (1992)
35. S. Jana, P.K. Biswas, Mater. Lett. **32**, 263 (1997)
36. P. Sharma, H.S. Bhatti, Mater. Chem. Phys. **114**, 889 (2009)
37. D.P. Yu, Q.L. Hang, Y. Ding, H.Z. Zhang, Z.G. Bai, J.J. Wang, Y.H. Zou, W. Qian, G.C. Xiong, S.Q. Feng, Appl. Phys. Lett. **73**, 3076 (1998)
38. J.H. Stathis, M.A. Kastner, Phys. Rev. B **35**, 2972 (1987)
39. C. Itoh, T. Suzuki, N. Itoh, Phys. Rev. B **41**, 3794 (1990)
40. H. Nishikawwa, T. Shiroyama, R. Nakamura, Y. Ohki, K. Nagasawa, Y. Hama, Phys. Rev. B **45**, 586 (1992)
41. D.P. Yu, Q.L. Hang, Y. Ding, Z.H. Zhang, Z.G. Bai, J.J. Wang, Y.H. Zou, W. Qian, G.C. Xiong, S.Q. Feng, Appl. Phys. Lett. **73**, 3076 (1998)
42. X.C. Wu, W.H. Song, K.Y. Wang, T. Hu, B. Zhau, Y.P. Sun, J.J. Du, Chem. Phys. Lett. **336**, 53 (2001)
43. K.H. Lee, H.S. Yang, K.H. Baik, J. Bang, R.R. Vanfleet, W. Sigmund, Chem. Phys. Lett. **383**, 380 (2004)
44. Z.Q. Liu, S.S. Xie, L.F. Sun, D.S. Tang, W.Y. Zhou, C.Y. Wnag, W. Liu, Y.B. Li, X.P. Zou, G. Wang, J. Mater. Res. **16**, 683 (2001)
45. G.W. Meng, X.S. Peng, Y.W. Wang, C.Z. Wang, X.F. Wang, L.D. Zhang, Appl. Phys. A **76**, 119 (2003)
46. S. Kar, S. Chaudhuri, Solid State Chem. **133**, 151 (2005)
47. D.P. Yu, Q.L. Hang, Y. Ding, H.Z. Zhang, Z.G. Bai, J.J. Wang, Y.H. Zou, W. Quian, G.C. Xiong, S.Q. Feng, Appl. Phys. Lett. **7**, 3076 (1998)
48. K.H. Lee, S.W. Lee, R.R. Vanfleet, W. Sigmund, Chem. Phys. Lett. **37**, 498 (2003)